Ultrafast silicon-based active plasmonics at telecom wavelengths

Jan N. Caspers,[1,2,*] Nir Rotenberg,[1] and Henry M. van Driel[1]

[1]*Department of Physics and Institute for Optical Sciences, University of Toronto, Toronto, M5S 1A7, Canada*
[2]*Institut für Angewandte Physik, Karlsruher Institut für Technologie (KIT), Wolfgang-Gaede-Strasse 1, D-76131 Karlsruhe, Germany*
n.caspers@utoronto.ca

Abstract: Using a gold/silicon grating coupler and modulating the silicon dielectric constant with 775 nm, 800 fs pump pulses we demonstrate an ultrafast spectral shift to a surface plasmon polariton coupling resonance for 1300-1700 nm probe pulses. With a modest pump fluence of 2.2 mJcm^{-2} the pump-induced free carriers shift the resonance by more than its width, with recovery occurring in 103 ps due to surface recombination.

OCIS codes: (230.4110) Modulators; (240.6680) Surface plasmons; (250.5403) Plasmonics; (320.7080) Ultrafast devices; (320.7085) Ultrafast information processing; (320.7110) Ultrafast nonlinear optics.

References and links

1. E. Ozbay, "Plasmonics: merging photonics and electronics at nanoscale dimensions," Science **311**(5758), 189–193 (2006).
2. W. L. Barnes, A. Dereux, and T. W. Ebbesen, "Surface plasmon subwavelength optics," Nature **424**(6950), 824–830 (2003).
3. J. A. Schuller, E. S. Barnard, W. Cai, Y. C. Jun, J. S. White, and M. L. Brongersma, "Plasmonics for extreme light concentration and manipulation," Nat. Mater. **9**(3), 193–204 (2010).
4. E. Hendry, F. J. Garcia-Vidal, L. Martin-Moreno, J. G. Rivas, M. Bonn, A. P. Hibbins, and M. J. Lockyear, "Optical control over surface-plasmon-polariton-assisted THz transmission through a slit aperture," Phys. Rev. Lett. **100**(12), 123901 (2008).
5. T. Nikolajsen, K. Leosson, and S. Bozhevolnyi, "Surface plasmon polariton based modulators and switches operating at telecom wavelengths," Appl. Phys. Lett. **85**(24), 5833 (2004).
6. A. L. Lereu, A. Passian, J.-P. Goudonnet, T. Thundat, and T. L. Ferrell, "Optical modulation processes in thin films based on thermal effects of surface plasmons," Appl. Phys. Lett. **86**(15), 154101 (2005).
7. R. A. Pala, K. T. Shimizu, N. A. Melosh, and M. L. Brongersma, "A nonvolatile plasmonic switch employing photochromic molecules," Nano Lett. **8**(5), 1506–1510 (2008).
8. D. Pacifici, H. Lezec, and H. Atwater, "All-optical modulation by plasmonic excitation of CdSe quantum dots," Nat. Photonics **1**(7), 402–406 (2007).
9. A. Y. Elezzabi, Z. Han, S. Sederberg, and V. Van, "Ultrafast all-optical modulation in silicon-based nanoplasmonic devices," Opt. Express **17**(13), 11045–11056 (2009), http://www.opticsinfobase.org/oe/abstract.cfm?URI=oe-17-13-11045.
10. K. MacDonald, A. Krasavin, and N. Zheludev, "Optical modulation of surface plasmon-polariton coupling in a gallium/aluminium composite," Opt. Commun. **278**(1), 207–210 (2007).
11. J. A. Dionne, K. Diest, L. A. Sweatlock, and H. A. Atwater, "PlasMOStor: a metal-oxide-Si field effect plasmonic modulator," Nano Lett. **9**(2), 897–902 (2009).
12. N. Rotenberg, M. Betz, and H. M. van Driel, "Ultrafast control of grating-assisted light coupling to surface plasmons," Opt. Lett. **33**(18), 2137–2139 (2008).
13. N. Rotenberg, J. N. Caspers, and H. M. van Driel, "Tunable ultrafast control of plasmonic coupling to gold films," Phys. Rev. B **80**(24), 245420 (2009).
14. K. F. MacDonald, Z. L. Sámson, M. I. Stockman, and N. I. Zheludev, "Ultrafast active plasmonics," Nat. Photonics **3**(1), 55–58 (2009).
15. D. J. Cho, W. Wu, E. Ponizovskaya, P. Chaturvedi, A. M. Bratkovsky, S.-Y. Wang, X. Zhang, F. Wang, and Y. R. Shen, "Ultrafast modulation of optical metamaterials," Opt. Express **17**(20), 17652–17657 (2009), http://www.opticsinfobase.org/oe/abstract.cfm?URI=oe-17-20-17652.
16. K. M. Dani, Z. Ku, P. C. Upadhya, R. P. Prasankumar, S. R. Brueck, and A. J. Taylor, "Subpicosecond optical switching with a negative index metamaterial," Nano Lett. **9**(10), 3565–3569 (2009).
17. H. Raether, *Surface Plasmons* (Springer, Berlin, 1988).
18. W. Barnes, "Surface plasmon–polariton length scales: a route to sub-wavelength optics," J. Opt. A, Pure Appl. Opt. **8**(4), S87–S93 (2006).
19. J. Pankove, *Optical Processes in Semiconductors* (Dover Publications, New York, 1975).

#131791 - $15.00 USD Received 22 Jul 2010; revised 18 Aug 2010; accepted 23 Aug 2010; published 1 Sep 2010

20. O. Madelung, *Semiconductors - Basic Data* (Springer, 1996).
21. Y. Vlasov, W. M. J. Green, and F. Xia, "High-throughput silicon nanophotonic wavelength-insensitive switch for on-chip optical networks," Nat. Photonics **2**(4), 242–246 (2008).
22. K. L. Luke, and L. Cheng, "Analysis of the interaction of a laser pulse with a silicon wafer: Determination of bulk lifetime and surface recombination velocity," J. Appl. Phys. **61**(6), 2282–2293 (1987).
23. S. Cristoloveanu, "Silicon films on sapphire," Rep. Prog. Phys. **50**(3), 327–371 (1987).

1. Introduction

The emergence of integrated information processing technologies based on surface plasmon polaritons (SPPs) has been gaining momentum as researchers come to understand and learn how to control these unique modes [1–3]. A cornerstone of this developing technology is the active control of the propagation [4–10] of, or the coupling [11–14] of light to, these polaritons. A key goal is a high contrast switching element that operates with minimal activation energy and on a picosecond time scale, making it compatible with multi-GHz technology.

SPPs, propagating electromagnetic fields coupled to electron oscillations at a metal-dielectric interface, combine the advantages of the high speed of light and nanometer mode confinement-scales that are usually associated with electronics. The use of plasmonic elements for integrated nanophotonic devices is therefore both intriguing and promising [1–3]. The first generation of active plasmonic elements, such as extraordinary transmission switches [4], plasmonic propagation modulators [5–7], or all-optical quantum-dot based plasmonic excitation [8] offer high contrast but suffer from slow recovery times and are incompatible with multi-GHz information processing technology. Subsequent schemes such as plasmon-mediated control of waveguide modes [9], MOSFET designs for plasmonic waveguides [10], opto-thermal modulation of plasmonic coupling on gold films at visible wavelengths [11–13], or optical control of SPP propagation on aluminium films near 780 nm through an interband resonance [14] are promising. These exhibit ultrafast active plasmonic control, yet are limited by either low modulation efficiencies or high pump fluence requirements. While such control has recently been shown in metamaterials [15,16] where the negative index of refraction resonance is quenched, there have been no similar reports based on work with plasmonics.

In this work, we demonstrate a silicon-based active plasmonic coupler with a picosecond scale recovery time, high contrast switching at telecom frequencies, and activation with low pump fluences. Additionally, as this approach is compatible with silicon processing technology, it represents an essential step towards next-generation plasmonic-based nanophotonic applications.

2. Theoretical background of active SPP coupling

Our modulator uses a silicon/gold grating to couple light to a SPP as shown in Fig. 1. Coupling requires matching the parallel component of the *k*-vectors of light and the SPP with the aid of the grating so that [17]

$$k_0 sin(\theta) + mG = k_{SPP}, \tag{1}$$

where k_0 is the vacuum wave vector, θ is the incident angle, m is an integer, and G is the grating reciprocal lattice vector. The SPP wavevector, k_{SPP}, depends on the relative dielectric function of both the gold and the silicon, $\varepsilon_{Si/Au}$, through [18]

$$k_{SPP} = k_0 \sqrt{\frac{\varepsilon_{Si}\varepsilon_{Au}}{\varepsilon_{Si} + \varepsilon_{Au}}}. \tag{2}$$

To modulate the coupling we optically inject free-carriers into the silicon with a pump pulse and alter its dielectric function due to Drude contributions [19]; these changes modify k_{SPP} and thus shift the wavelength at which resonant light-SPP coupling occurs.

#131791 - $15.00 USD Received 22 Jul 2010; revised 18 Aug 2010; accepted 23 Aug 2010; published 1 Sep 2010

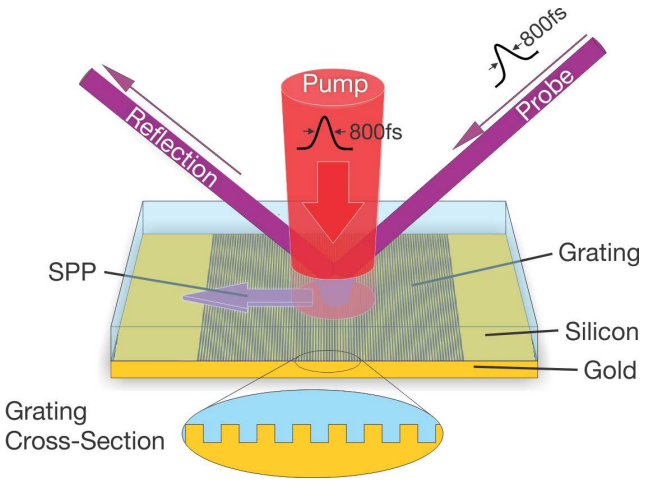

Fig. 1. Schematic of the active grating coupler. A grating at a silicon-gold interfaces couples light from a p-polarized probe pulse to a SPP. The coupling is modulated by a 775 nm pump pulse that induces free carriers in the silicon. The sapphire layer on top of the silicon has been removed for clarity.

We estimate the changes to k_{SPP} by calculating the carrier induced changes to ε_{Si}. In the experiments discussed below (see Fig. 1) we use a 0.5 µm thick layer of silicon pumped by a pulse centered at 775 nm, for which the absorption depth is ~9 µm. If we reasonably consider that absorption is dominated by interband absorption (silicon band gap: 1.1 eV [20]), the injected free-carrier density, N_c, is proportional to the pump fluence. For a fluence of 1 mJcm^{-2} we estimate $N_c \sim 1\times 10^{19}$ cm^{-3} throughout the thin Si film with only ~6% of the incident light absorbed; the remaining light is reflected and could possibly be used to activate additional systems. The Drude changes to the dielectric function for a probe beam are given by [19]

$$\Delta\varepsilon = -\frac{\omega_p^2}{\omega^2 + i\gamma\omega}, \tag{3}$$

where γ is the carrier collision rate (~10 THz [20]), ω is the probe frequency and ω_p is the bulk plasma frequency defined as

$$\omega_p = \sqrt{\frac{N_c q^2}{\varepsilon_0 m^*}}. \tag{4}$$

Here q is the elementary charge and m^* as the reduced effective mass of electron and holes (~0.4 m_0, where m_0 is the free electron mass [20]). Figure 2 shows the changes to the complex relative dielectric function and the induced shifts for two SPP resonances originally centered at 1400 and 1550 nm; the grating period is 500 nm. As expected, the changes to the dielectric function, and consequently the shifts, increase with increasing wavelength.

Since the FWHM of plasmonic coupling resonances is typically ~30-50 nm, we predict that this scheme leads to spectral shifts of the resonance greater than its width for modest fluences. Although this is demonstrated here for telecom wavelengths, since the Drude contribution to the dielectric function increases with increasing wavelength [19], this approach to SPP control is applicable over the near and mid infrared.

#131791 - $15.00 USD Received 22 Jul 2010; revised 18 Aug 2010; accepted 23 Aug 2010; published 1 Sep 2010

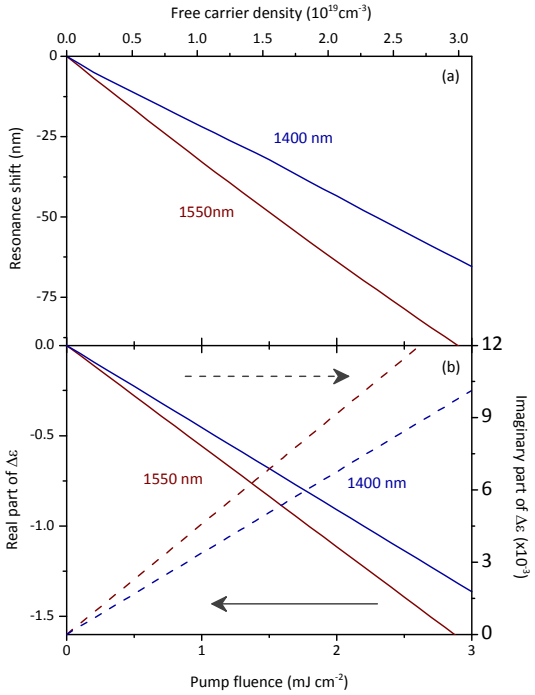

Fig. 2. Simulation of the induced changes to silicon dielectric function and shift of the SPP resonance for a grating with $2\pi / G$ = 500 nm. (a) The spectral shift of SPP resonances that are originally centered at 1400 nm (blue) and 1550 nm (red) as a function of pump fluence and induced free carrier density. (b) The changes to both the real part (solid line, left axis) and the imaginary part (dashed line, right axis) of the relative dielectric function of silicon at 1400 nm (blue) and 1550 nm (red) as a function of incident pump fluence and free carrier density.

3. Experimental setup and sample fabrication

The plasmonic coupling modulator was fabricated using a commercially available silicon on sapphire (SOS) wafer. The silicon side was patterned with electron-beam lithography, and wet etched with potassium hydroxide (KOH). The resultant square grating structure (500 μm by 500 μm) has a period of 500 nm and a nominal depth of 70 nm. A monolayer of chromium, was deposited for adhesion purposes, followed by a 170 nm layer of gold, completing the fabrication. One exemplary sample was cut and analysed by a SEM to verify the grating profile and gold layer thickness.

A commercial Ti:sapphire amplifier pumping an OPA generates 800 fs (FWHM) probe pulses, with center wavelengths between 1300 nm and 1700 nm, and 20 nm spectral bandwidth (FWHM). These pulses are used as a probe, passing through the silicon-sapphire system and incident on the grating where they couple to SPPs (Fig. 1). We measure a spot size of 100 μm using a "knife-edge" technique on the grating. The presence of the plasmonic coupling resonances is confirmed by measuring the zero-order reflectivity of the sample for different incident probe beam angles. As expected, the spectral dip in the p-polarized reflectivity shifts with angle, as seen in Fig. 3. While not shown here, the s-polarized reflectivity spectrum is featureless, as expected.

As shown in Fig. 1, the plasmonic coupling is modulated by an 800 fs (FWHM), 775 nm pump pulse that is normally incident on the silicon. We use pump fluences up to 2.2 mJcm^{-2} on a 500 μm spot size (5× the probe spot size). Because the coupling of the probe light to a SPP is intimately dependent on the dielectric function [18], the pump-induced increase of the Drude contribution results in a change to the probe-SPP coupling condition. We monitor the

#131791 - $15.00 USD Received 22 Jul 2010; revised 18 Aug 2010; accepted 23 Aug 2010; published 1 Sep 2010

changes in the probe reflectivity spectrum as a function of delay time between probe and pump pulse; from this we deduce the changes in the coupling efficiency.

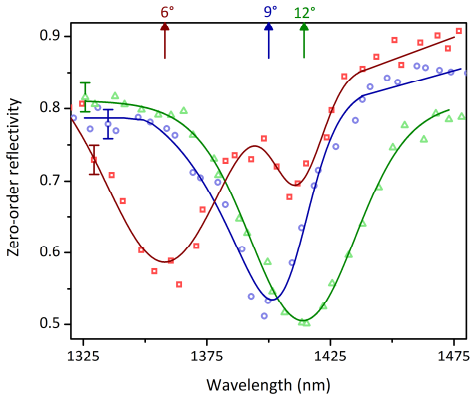

Fig. 3. Angle dependent SPP excitation. Zero-order reflectivity spectra for 6°, 9°, and 12° incident angles at the silicon-gold interface show different SPP resonances. The small dip near 1415 nm for the 6° curve is due to a Wood-Rayleigh anomaly. The symbols represent the measured values and the curves are guides to the eye.

4. Results and discussion

4.1 Ultrafast plasmonic coupling dynamics

Figure 4a shows the zero-order probe reflectivity spectrum for a pump fluence of 2 mJcm^{-2}. Initially, the SPP resonance is seen as a large dip in reflectivity centered near 1400 nm, with a FWHM of 38 nm. At a time delay of 3.3 ps the resonance shifts to 1360 nm, but then slowly relaxes back to 1400 nm; by 130 ps, a time related to carrier recombination (see below), the system has almost completely recovered. The reflection spectrum at 3.3 ps also shows a second dip in reflectivity for wavelength above 1420 nm; this reflects coupling to a second plasmon resonance that is centered near 1550 nm in the unexcited material, and which also shifts due to the excitation of the silicon.

The transient reflectivity curves shown in Fig. 4b exemplify the dynamics of the SPP resonance, and, in particular, the interplay between its shift and free carrier alteration of the silicon dielectric function. We mark four points (A,B,C,D) on the transient curve at 1370 nm (corresponding to the four curves in Fig. 4a) that show this behavior. At point "A" there are no changes before the pump arrives while at "B" the SPP resonance has shifted to shorter wavelengths, reaching 1370 nm at a time delay of ~1 ps (see inset to Fig. 4b). The resonance then continues to shift, reaching ~1360 nm before starting to relax back to 1400 nm; this is revealed by the sharp dip in the reflectivity shown in both the inset and main part of Fig. 4b at 1 ps, followed by the slow recovery of the reflectivity.

The overshoot of the resonance is more obvious on the 1390 nm curve where the reflectivity first sharply decreases then increases as the center of the resonance passes this wavelength, then slowly decreases until the resonance is once again centered at 1390 nm for a delay of 80 ps. Lastly, the reflectivity slowly increases as the plasmon resonance shifts past 1390 nm and returns towards 1400 nm. The change in the reflectivity is never positive in this case due to free carrier absorption, though it can be for other pump fluences (not shown). This happens when the resonance shifts sufficiently but the absorption due to the free carriers is still relatively small. Points "C" and "D" show the recovery of the reflectivity as the SPP resonance shifts back to its original position.

#131791 - $15.00 USD Received 22 Jul 2010; revised 18 Aug 2010; accepted 23 Aug 2010; published 1 Sep 2010

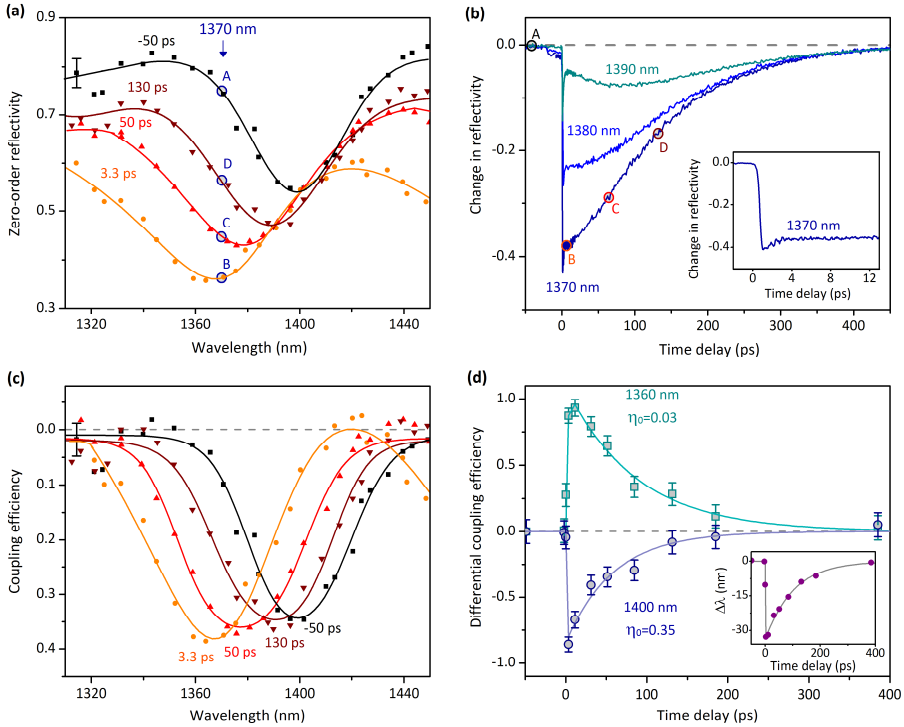

Fig. 4. Probe reflectivity and plasmonic coupling dynamics. (a) Zero-order reflectivity spectra for different delay times. The A,B,C, D letters indicate the order in time. The symbols are the measured values and the curves are guides to the eye. (b) The change in reflectivity as a function of time delay for 3 different wavelengths on the short wavelength side of the SPP resonance. The circles with the letters indicate the time delays that correspond to the reflectivity curves shown in (a). The inset shows the behaviour at 1370 nm for small time delays after the temporal overlap of pump and probe pulses. (c) The coupling efficiency as a function of wavelength for the same time delays as in (a). (d) The differential coupling efficiency (the modulation of the coupling efficiency normalized to the original coupling efficiency at 1400 nm) as a function of delay time. The inset shows the shift of the SPP center wavelength as a function of delay time.

The effectiveness of the Si-Au modulator is more evident from a consideration of the plasmonic coupling efficiency, which is defined as the amount of energy coupled from the incident light to a SPP. The plasmonic coupling efficiency is calculated by taking the difference between the spectrum with dip and a featureless background spectrum. The coupling efficiency is shown for different time delays in Fig. 4c corresponding to the reflectivity shown in Fig. 4a. Here, both the initial shift of the plasmonic resonance and the slow relaxation are evident, as is the fact that the change to the optical properties of the silicon does not decrease the amplitude of the SPP resonance. From these curves we extract the change to the SPP coupling efficiency, and normalize it to the initial coupling efficiency at the center of the resonance (~0.35).

Figure 4d shows the changes to the coupling efficiency at the unperturbed resonance center wavelength, 1400 nm, and at its wings at 1360 nm, as a function of time delay. The spectral shift of the plasmonic resonance is shown for the same time delays in the inset. Shortly after temporal overlap of pump and probe pulses we observe modulation of –91% and + 93% at 1400 nm and 1360 nm, respectively. Initially the plasmonic coupling efficiency is 0.35 and 0.03 at 1400 nm and 1360 nm, respectively, and due to the pump-induced changes to the dielectric function these become 0.03 and 0.36, respectively. That is, the resonance is effectively shifted from 1400 nm to 1360 nm. In fact, the plasmonic resonance shifts to

#131791 - $15.00 USD Received 22 Jul 2010; revised 18 Aug 2010; accepted 23 Aug 2010; published 1 Sep 2010

shorter wavelengths by 32 nm, which is 5 times larger than the shift observed due to electron thermal effects in gold in a PMMA/gold grating [13]; this is particularly exciting since the fluence used here is also 30 times lower. We note that the magnitude of the initial coupling efficiency is dependent on excitation geometry. Since plasmonic grating couplers can be optimized to > 0.9 efficiency [17], and since the modulations observed here are not dependent on the amplitude of the plasmon resonance but rather on its shift, the approach presented here can be used to effectively modulate highly efficient couplers.

We also use the shift to estimate the number of induced free carriers. Using Eqs. (1-4) we calculate that a carrier density of $\sim 1.5 \times 10^{19}$ cm^{-3} (corresponding to a pump fluence of ~1.5 mJcm^{-2}) is required to shift the plasmonic resonance by 32 nm (Fig. 2). Recall that a pump fluence of 2 mJcm^{-2} is measured (corresponding to $N_c \sim 2 \times 10^{19}$ cm^{-3}), which, to within the errors in the measurement, is in good agreement with the calculated value. We note that the carrier density required for switching in our scheme is comparable to that required by recent silicon-based optical switches [21].

To characterize the dynamics for the plasmonic coupler we fit an exponential curve to both the transient differential coupling efficiency and to the resonance shift. The extracted characteristic recovery times are 60 ± 8 ps for the differential coupling efficiency and 103 ± 5 ps for the SPP resonance shift; the differential coupling efficiency recovers faster than the SPP shift as it is a function of both the real and imaginary changes to the dielectric function and the spectral shape of the resonance. To determine the actual carrier recombination time pump-probe reflectivity experiments were carried out on an unstructured part of the sample, from which we extract a recombination time of 70 ± 8 ps on the planar surface. Suprisingly, this value is smaller than the decay constant of the shift. We attribute this difference to the fact that the free-carrier decay measurements are performed on an unstructured part of the sample, in contrast with the plasmonic measurements, and as we discuss below, surface effects dominate the decay dynamics of our system. The fast decay constant contrasts with millisecond recombination times in very pure bulk silicon [22], but is not unexpected in thin films where surface recombination plays a strong role; in this system, both the gold-silicon and sapphire-silicon interfaces have a high surface recombination velocity [23]. Note that the recombination time could be further reduced by adding defects to the silicon, e.g., through ion implantation.

4.2 Fluence dependence

We further characterize the active SPP coupler by measuring the reflectivity spectrum with the initial resonance at 1400 nm and varying the pump fluence between 1 and 2.2 mJcm^{-2}. Figure 5 summarizes both the shift of the center of the plasmonic resonance normalized to its FWHM (~38 nm), as well as the peak modulation of the coupling efficiency at the center of the resonance (1400 nm), as functions of the pump fluence. We observe a maximum spectral shift of −1.2 times the FWHM of the resonance for the modest pump fluence of 2.2 mJcm^{-2}.

The dependence of the peak modulation of the coupling efficiency at 1400 nm (Fig. 5, right-axis) on the pump fluence shows three distinct regions. First, for fluences below ~1.4 mJcm^{-2} the modulation increases rapidly with increasing fluence due to both large shifts and the presence of free carrier absorption. For fluences between 1.4 mJcm^{-2} and 2.0 mJcm^{-2} the modulation slowly increases from ~0.9, as the resonance shift is sufficiently large that the original center, at 1400 nm, is located on the tail of the shifted resonance. Finally, for even larger pump fluences, the resonance shift is so large that there is no coupling and the modulation increases to, and plateaus at a value near unity; we see this clearly for a pump fluence of 2.2 mJcm^{-2}.

#131791 - $15.00 USD Received 22 Jul 2010; revised 18 Aug 2010; accepted 23 Aug 2010; published 1 Sep 2010

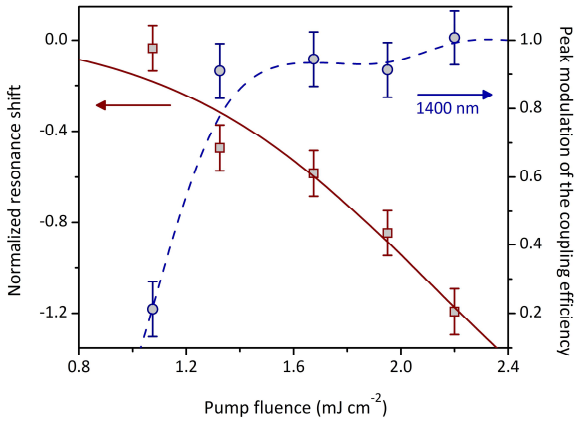

Fig. 5. The pump fluence dependency of the plasmonic shifts and modulations. The normalized resonance shift (left axis, red curve), the maximum spectral shifts divided by the FWHM of the resonance, and the peak modulation of the coupling efficiency (right axis, blue curve) at 1400 nm are shown as a function of the pump fluence. The symbols represent the measured values and the curves are guides to the eye.

5. Conclusions

We have presented an active silicon-based plasmonic coupler and shown that for wavelength near 1400 nm the center of the plasmonic resonance can be optically shifted by more than its FWHM, resulting in high-contrast switching. We have observed similar behavior for coupling resonances near 1550 nm, found by changing the angle of incidence, as shown in Fig. 3. This tunability is expected as the nature of free carrier effects is broad-band. For modulation of longer wavelengths than given here the pump requirements will drop along with the required free carrier density, although free carrier absorption effects will become more important. With a careful choice of the grating and incident geometry, the plasmonic coupling at a given wavelength can be switched off, as was demonstrated here at 1400 nm, or it can be switched on, as we saw at 1360 nm.

Switching times on the order of picoseconds have been obtained making multi-GHz applications feasible. The modest pump fluence required to achieve switching is an order of magnitude lower than that used for previous ultrafast modulation schemes [13,14], and even for those techniques where slower switching times ranging from nanoseconds to picoseconds were obtained [4–8]. The energy demands of this technique compare favorably with current optical technology, and are much smaller than those required to digitally encode information on a compact disc. Lastly, the modulator's materials – silicon and gold – are compatible with current chip manufacturing, making an implementation of a nanophotonic device based on the observed process easy.

The performance of this modulator has not been optimized. In particular, the required fluence and the switching times can be reduced in a number of ways. First, the grating can be optimized to make the resonance narrower and increase the coupling at the center. Hence the resonance would not need to shift as much as given here, reducing the required fluence. Second, the silicon film thickness can be reduced since the SPP only penetrates into the silicon by ~100 nm [18]. Third, amorphous silicon can be used instead of crystalline silicon to increase the absorption coefficient and thus further decrease the required fluence. Due to the larger number of defects in amorphous silicon, carrier recombination and switching times would also be smaller. Another option to decrease the fluence requirements is to pump Si at

#131791 - $15.00 USD Received 22 Jul 2010; revised 18 Aug 2010; accepted 23 Aug 2010; published 1 Sep 2010

shorter wavelengths, closer to the direct band gap (~350 nm), further decreasing the absorption depth.

Overall, this modulator concept can serve as a practical active plasmonic element in an integrated next-generation information processing application, across a broad band of wavelengths, including the important telecom wavelengths.

Acknowledgements

We acknowledge funding by the Natural Science and Engineering Research Council of Canada.

#131791 - $15.00 USD Received 22 Jul 2010; revised 18 Aug 2010; accepted 23 Aug 2010; published 1 Sep 2010